

Early warning signal for interior crises in excitable systems

Rajat Karnatak*

Leibniz-Institute of Freshwater Ecology and Inland Fisheries, Müggelseedamm 310, 12587, Berlin, Germany

Holger Kantz[†] and Stephan Bialonski[‡]

Max Planck Institute for the Physics of Complex Systems, Nöthnitzer Straße 38, 01187 Dresden, Germany

The ability to reliably predict critical transitions in dynamical systems is a long-standing goal of diverse scientific communities. Previous work focused on early warning signals related to local bifurcations (critical slowing down) and non-bifurcation type transitions. We extend this toolbox and report on a characteristic scaling behavior (critical attractor growth) which is indicative of an impending global bifurcation, an interior crisis in excitable systems. We demonstrate our early warning signal in a conceptual climate model as well as in a model of coupled neurons known to exhibit extreme events. We observed critical attractor growth prior to interior crises of chaotic as well as strange-nonchaotic attractors. These observations promise to extend the classes of transitions that can be predicted via early warning signals.

PACS numbers: 05.45.-a, 05.45.Tp, 89.90.+n, 87.19.1l, 92.70.Aa

The dynamical behavior of many complex systems can undergo dramatic changes. Such critical transitions have been associated with a multitude of complex systems that are important to human societies, ranging from potentially devastating transitions in the earth's climate system due to climate change [1], regime shifts such as desertification or eutrophication phenomena in ecosystems [2–4], to the progression into chronic disease states in humans (such as depression, inflammation, or cardiovascular disease) [5]. Reliable and early predictions of critical transitions are very desirable and would not only allow for a warning of an impending event but also for time to prepare and to develop countermeasures.

Research that focusses on early warning signals for critical transitions associated with bifurcations (*B-tipping* [6]) has gained strong momentum during the past years [7, 8], notably studies concentrating on the phenomenon of “critical slowing down” (CSD) [9]. CSD manifests in slow rates of recovery from small perturbations near *local* bifurcations, resulting in an increased variance and lag-1 autocorrelation in the time series of appropriate observables. CSD can be traced back to the fact that in local bifurcations, the dominant eigenvalue(s) of the Jacobians associated with equilibria or cycles smoothly approach(es) zero or the unit circle (leading to neutral/marginal stability), thereby slowing down and ultimately preventing the decay of perturbations at the bifurcation point. While CSD has been demonstrated experimentally for different systems, including yeast populations [10] and food webs in lakes [11], it has also been repeatedly pointed out to fail as an early warning signal if transitions are not associated with local bifurcations [3, 7, 12, 13]. Indeed, from a *B-tipping* perspective, global bifurcations such as crises [14, 15], which involve

larger and more complex invariant sets compared to local bifurcations, are usually not tractable using local stability properties of equilibria and/or cycles. Thus, they are typically not revealed by CSD.

In this contribution, we demonstrate an early warning signal that is sensitive to a global bifurcation, namely an interior crisis in excitable systems. We consider crises in a conceptual climate model [16] as well as in a system of coupled FitzHugh–Nagumo units [17, 18]. In both systems, we observe a characteristic scaling behavior to indicate an impending crisis, i.e. a sudden increase in the size of an attractor. In a second step, we exploit this scaling behavior in order to predict a crisis and, as a consequence, the onset of *crisis-induced intermittency* [19] (post-crisis). In excitable systems, the latter has been associated with dynamical regimes that can exhibit extreme events [17, 18, 20].

We consider the following two excitable systems to demonstrate the predictability of an interior crisis:

- System 1: Two mutually coupled FitzHugh–Nagumo oscillators as studied in Refs. [17, 18],

$$\begin{aligned}\dot{x}_i &= x_i(a - x_i)(x_i - 1) - y_i + \kappa_1(x_j - x_i), \\ \dot{y}_i &= b_i x_i - c y_i,\end{aligned}\tag{1}$$

where x_i and y_i correspond to the excitatory and inhibitory variables respectively, and $i, j \in \{1, 2\}, i \neq j$. Furthermore, let $\bar{x}(t)$ denote the arithmetic mean of the excitatory variables, $\bar{x}(t) = (x_1(t) + x_2(t))/2$. The coupling strength κ_1 was varied in our numerical studies, whereas the remaining parameters were fixed ($a = -0.025794$, $c = 0.02$, $b_1 = 0.0135$, $b_2 = 0.0065$).

- System 2: Dimensionless form of a conceptual cli-

* karnatak@igb-berlin.de

† kantz@pks.mpg.de

‡ bialonski@gmx.net

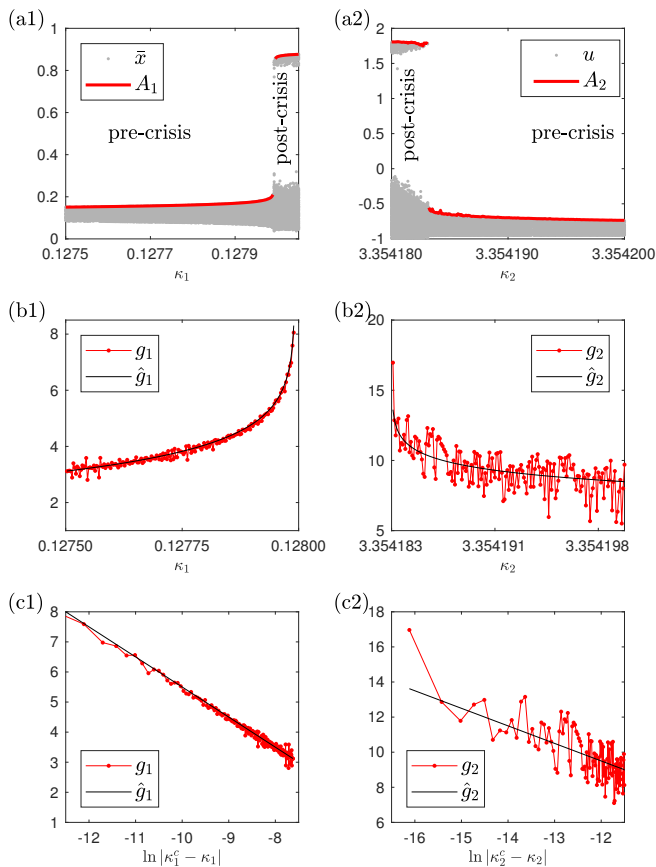


FIG. 1. Bifurcation diagrams of System 1 (a1) and System 2 (a2). For each value of κ_1 and κ_2 , grey points mark local maxima of a time series ($\bar{x}(t)$ and $u(t)$, respectively) and red (dark) points denote the respective global maximum values, $A_1(\kappa_1)$ and $A_2(\kappa_2)$, determined from ensembles of time series (20 initial conditions, 10^5 time units per time series for System 1; 10^3 initial conditions, 10^7 time units per time series for System 2; initial 10^5 (System 1) and 10^6 (System 2) time units were discarded as transients). Pre- and post-crisis regimes are marked by text labels. Parameter regimes of $\kappa_1 \in [0.1275, 0.12805]$ and $\kappa_2 \in [3.35418, 3.3542]$ were sampled in step sizes of $\delta\kappa_1 = 2.75 \times 10^{-6}$ and $\delta\kappa_2 = -1.0 \times 10^{-7}$, respectively. The set of equations (1) and (2) were solved numerically using the VODE package [21]. Panels (b1) and (b2) show logarithmic growth rates (red-dotted curves) g_1 and g_2 as defined in equation (3) in the pre-crisis regimes of Systems 1 and 2 (i.e. $\kappa_1 \in [0.1275, \kappa_1^c - \delta\kappa_1]$, $\kappa_2 \in [\kappa_2^c + \delta\kappa_2, 3.3542]$). The same data is shown as functions of the logarithm of the parametric distance from the critical values, $\ln|\kappa_i^c - \kappa_i|$, in panels (c1) and (c2) respectively. Lines \hat{g}_1 and \hat{g}_2 (black lines in panels (c1) and (c2)) were fitted to the data with a fixed slope of -1 . These fits are also shown as black curves in panels (b1) and (b2).

mate model [16],

$$\begin{aligned} \dot{u} &= \epsilon^{-1} (v - u^3 + 3u - k), \\ \dot{v} &= p(u - a)^2 - \kappa_2 - mv - (\lambda + v) + w, \\ \dot{w} &= r(\lambda + v - w), \end{aligned} \quad (2)$$

where the variable u is related to the continental ice volume offset from a mean value, v relates to the amount of carbon in the atmosphere, and w to the amount of carbon in the mixed layer of the ocean. We varied parameter κ_2 , while the remaining parameters were fixed at suitable values ($\epsilon = 0.1$, $a = 0.8$, $p = 3$, $k = 4$, $r = 0.05$, $m = 1$, $\lambda = 1$; see Ref. [16]).

To demonstrate the characteristic scaling prior to crises in these systems, we show bifurcation diagrams of System 1 and System 2 in panels (a1) and (a2) of figure 1. In both diagrams, for each fixed parameter values of κ_1 and κ_2 , red (dark) points represent maximum values A_1 and A_2 of \bar{x} and $u(t)$, respectively, determined from ensembles of time series of different initial conditions. In System 1 (panel (a1)), the size of a chaotic attractor resulting from a period doubling route to chaos increases with increasing κ_1 values; the attractor undergoes an interior crisis. In System 2 (panel (a2)), a strange non-chaotic attractor which mediates a quasiperiodic route to chaos experiences an interior crisis for decreasing κ_2 values (similar to “route A” as described in Ref. [22]). In both cases, we observe A_1 and A_2 to show a steady growth as we approach the interior crisis, before exhibiting a discontinuous transition to high values beyond the critical values $\kappa_1^c \approx 0.1279922$ and $\kappa_2^c \approx 3.3541833$.

To quantify the growth of the attractors for both systems in the pre-crisis regimes, we determine the logarithmic growth rate,

$$g_i(\kappa_i) = \ln \left(\frac{A_i(\kappa_i + \delta\kappa_i) - A_i(\kappa_i)}{|\delta\kappa_i|} \right), \quad (3)$$

where $i \in \{1, 2\}$ and $\delta\kappa_i$ are small increments of κ_i (see caption of figure 1). The numerically determined growth rates g_1 and g_2 (panels (b1) and (b2) of fig. 1; red-dotted lines) of both systems for the pre-crisis regimes show a consistent increase with increasing proximity to the critical values. This proximity-dependent behavior becomes even more apparent if these growth rates are shown as functions of the logarithm of the parametric distance from the critical values, $\ln|\kappa_i^c - \kappa_i|$, in panels (c1) and (c2) [red dotted lines]. Indeed, these results suggest a linear scaling (with a slope of approximately -1 for our systems) between g_i and the logarithmic parametric distances,

$$g_i(\kappa_i) \propto \ln|\kappa_i^c - \kappa_i|. \quad (4)$$

We fitted lines \hat{g}_1 and \hat{g}_2 with a slope of -1 to the data in panels (c1) and (c2). These fits are shown as black curves in panels (b1)-(c2) and agree well with the observed data.

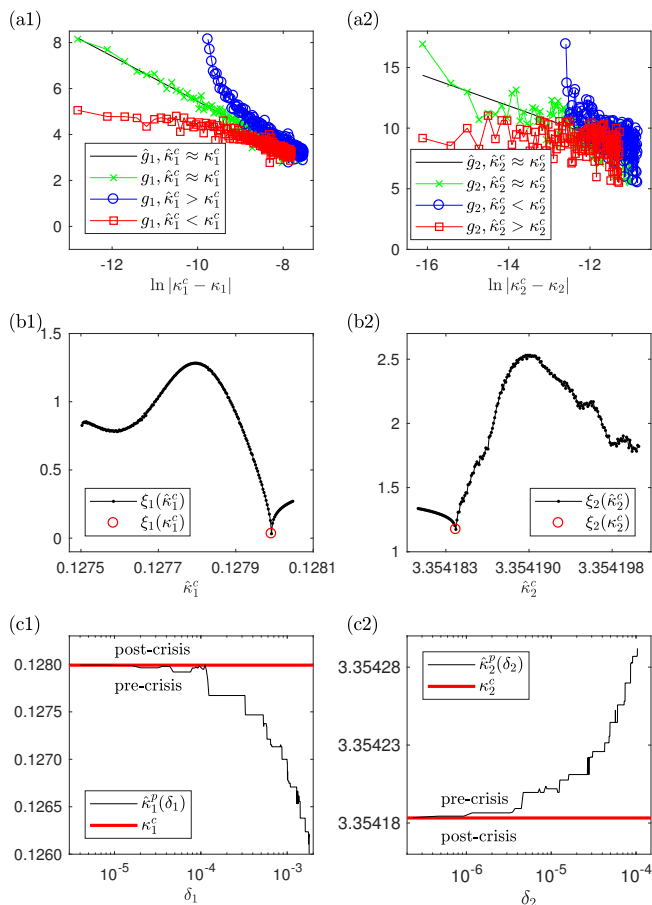


FIG. 2. Logarithmic growth rates g_1 (a1) and g_2 (a2) as determined by equation (3) for values of κ_1 and κ_2 from the pre-crisis regimes of Systems 1 and 2, respectively. The growth rates are shown as functions of the logarithmic parametric distances to the candidate critical values $\hat{\kappa}_i^c$ of the systems. To determine growth rates, the ensembles of time series of figure 1 were used. Different curves of g_i are shown color-and-symbol coded and were obtained by varying the candidate critical values (red curves: $\hat{\kappa}_1^c = 0.127909$, $\hat{\kappa}_2^c = 3.35418$; blue curves: $\hat{\kappa}_1^c = 0.128047$, $\hat{\kappa}_2^c = 3.3541873$). Black lines denote linear fits to the curves for $\hat{\kappa}_i^c \approx \kappa_i^c$. The slopes of the best fits yielded -0.983 and -1.190 , respectively, which is in approximate agreement with -1 as empirically observed in figure 1. (b1), (b2) Dependence of the mean squared errors ξ_i of the linear fits on the candidate critical values $\hat{\kappa}_i^c$. Smallest errors were observed for those candidate critical values that equaled the actual critical values (marked by red circles). (c1), (c2) Dependence of the predicted critical values $\hat{\kappa}_i^p$ (narrow black lines) on the distance δ_i of the set of observed parameters with respect to the actual critical values κ_i^c (thick red lines). For each value of δ_i , the sets J_i of observed parameters were created as $J_i = [\nu_i, \nu_i + \delta\tilde{\kappa}_i, \dots, \nu_i + 49\delta\tilde{\kappa}_i]$, respectively, where $\nu_{1/2} = \kappa_{1/2}^c \mp \delta_{1/2}$, $\delta\tilde{\kappa}_1 = -4 \cdot 10^{-6}$, and $\delta\tilde{\kappa}_2 = 2.34 \cdot 10^{-7}$.

Can we predict an interior crisis prior to its occurrence by capitalizing on the scaling behavior? As stated before, crisis-induced intermittency [19] has been recently interpreted with respect to dynamical regimes that allow for the occurrence of extreme events [17, 18]. In this con-

text, predicting an interior crisis would mean to predict the transition into a dynamical behavior which exhibits extreme events. To study whether an interior crisis can be predicted, we assumed that we do not know the actual values of κ_1^c and κ_2^c ; and we considered only data that was observed in the pre-crisis regimes (cf. figure 1). Let $\hat{\kappa}_1^c$ and $\hat{\kappa}_2^c$ denote our guesses of the critical values (from now on called “candidate critical values”). In panels (a1) and (a2) of figure 2, we show the growth rates g_i (as defined by equation (3)) as functions of the logarithmic parametric distance from the candidate critical values $\hat{\kappa}_i^c$ for System 1 and 2, respectively. For different candidate critical values of $\hat{\kappa}_i^c$, we obtained different curves. When the candidate critical values were located in the actual pre-crisis regimes ($\hat{\kappa}_1^c < \kappa_1^c$, $\hat{\kappa}_2^c > \kappa_2^c$), the growth rates g_i did not show a linear scaling relationship with respect to the logarithmic distance to the candidate critical values. Instead, we observed concave downward curves (red curves with squares in panels (a1) and (a2)). As $\hat{\kappa}_i^c$ approached the actual critical values, we observed a transition from concave downward curves to a linear scaling behavior (with a slope of approximately -1 ; green crossed curves in panels (a1) and (a2)) for $\hat{\kappa}_i^c$ arbitrarily close or equal to the actual critical values. In addition, we show linear fits \hat{g}_i (black lines) in both panels that emphasize the linear scaling behavior when $\hat{\kappa}_i^c \approx \kappa_i^c$. When the candidate critical values were further changed and entered the actual post-crisis regime, we observed concave upward curves (blue curves with circles in panels (a1) and (a2)).

We built upon these observations to predict the actual crises values—having observed only the dynamics in the pre-crisis regimes—as follows. For ranges of κ_i of the pre-crisis regimes of both systems, we determined the logarithmic growth rates $g_i(\kappa_i)$ (see Eq. (3)). We then consider intervals of candidate critical values, $\hat{\kappa}_1^c$ and $\hat{\kappa}_2^c$, which are shown as abscissae in panels (b1) and (b2), respectively. For each candidate critical value $\hat{\kappa}_i^c$ of the interval, we consider the growth rate g_i as a function of the logarithmic distance between $\hat{\kappa}_i^c$ and κ_i and fitted a line. The mean squared error ξ_i of this fit and its dependence on the candidate critical value is shown in (b1) and (b2). Both panels complement the previous observations: We observed the mean squared errors to become minimal (within the investigated intervals) when the candidate critical values equaled the actual critical values (marked as red circles in both panels). The linear scaling behavior revealed the actual critical values.

The accuracy of the prediction of the critical value will depend on various factors such as the set of control parameters for which the system dynamics was observed (from now on called “observed parameters”). In particular, we hypothesized our predictions to become more accurate the closer the observed parameters are to the actual critical value. To study this hypothesis, we created a set J of observed parameters, consisting of 50 equidistantly spaced control parameter values in the pre-crisis regime. With δ_i we denote the minimum distance

between the actual critical value for System i and any of the observed parameters of the set. Furthermore, we created a set of candidate critical values. For each of the candidate critical values, we considered the growth rates g_i as a function of the logarithmic distance between the candidate critical value and $\kappa_i \in J$ and fitted a line. We predicted the critical value by determining the candidate critical value $\hat{\kappa}_i^c$ for which the mean squared error ξ of this fit was the smallest. Let $\hat{\kappa}_i^p$ denote this predicted value. We repeated this procedure for different sets J which we created by adding a small value ($\delta\hat{\kappa}_i$) to all members of the previous set, thereby yielding sets of observed parameters with different distances δ_i to the actual critical value.

In figure 2 (c1) and (c2), we show the dependence of the predicted critical values on the distance of the set of observed parameters. Indeed, for small distances δ_i , we observed the predicted values to be very close to the actual critical values. Increasing δ_i and thus observing the dynamics for control parameters that are more distant from the actual critical values ($\delta_1 > 10^{-4}$, $\delta_2 > 3.5 \cdot 10^{-6}$), we observed our predicted critical values to increasingly deviate from the actual ones, tending towards the pre-crisis regime. Consequently, in our numerical experiments, the probability to falsely locate the transition in the actual post-crisis regime (and thus risking to enter such a regime without warning) is marginal. These results underline that the predictions of an interior crisis become more accurate the closer we observe our dynamics with respect to the transition, an observation also reported with respect to local bifurcations and abrupt monsoon transitions [23].

The dynamics we considered so far were purely deterministic, a property that is not ubiquitously present in systems investigated in the field. In field studies, measurements may be contaminated by noise contributions and the investigated dynamics itself may contain stochastic components (for instance, consider biological systems and the intrinsic stochastic nature of involved processes). While increasing levels of measurement noise will likely decrease the parameter regime before the crisis for which we can reliably predict the critical transition (due to noise masking the maximum amplitudes), the effect of stochastic components present in the system dynamics on our prediction abilities could be non-trivial. To study this question, we added a Gaussian white noise term η to the first rate equation of System 1 and refer to this “noisy” system as System 1’, $\dot{x}'_1 = x'_1(a - x'_1)(x'_1 - 1) - y_1 + \kappa_1(x_2 - x'_1) + \sigma\eta(t)$, where σ^2 is the noise strength. Like for Systems 1 and 2, we observed a linear scaling behavior of the growth rate with respect to the logarithmic parametric distance (cf. figure 3(a), $\sigma = 10^{-4}$) when the candidate critical value was equal or arbitrarily close to the actual critical value. This scaling behavior allowed us to predict the critical transition even in System 1’, a result highlighting the robustness of our reported scaling characteristic.

The actual critical value in System 1’ is smaller than the critical value in System 1 (for $\sigma > 0$) and decreases

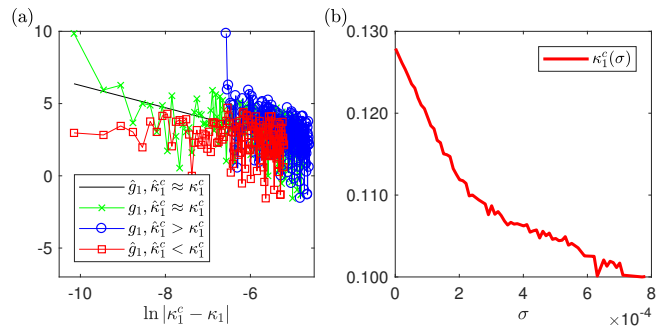


FIG. 3. (a) Logarithmic growth rate g_1' for values κ_1' of the pre-crisis regime of System 1’ with noise level $\sigma = 10^{-4}$. g_1' scales approximately linearly with the logarithmic parametric distance between the actual crisis value κ_1' and candidate critical values κ_1^c , (green crossed line: $\kappa_1^c \approx 0.118593$; black continuous line: linear fit with slope -0.771). Candidate critical values below (above) the actual critical yield concave downward (upward) curves with $\hat{\kappa}_1^c \approx 0.115469$ ($\hat{\kappa}_1^c \approx 0.119961$). System 1’ was numerically solved using the Euler-Maruyama method (step size $\delta t = 0.001$). For each values $\kappa_1' \in [0.11, 0.12]$ (step size $\delta\kappa_1' \approx 3.90625 \times 10^{-5}$), an ensemble of 5×10^3 initial conditions was created and evolved for 4×10^8 time units. The initial 10^8 time units were evolved without noise and discarded as transients. From the ensemble, the global maximum amplitude (of the mean value \bar{x}' of both excitatory variables of System 1’) which enter equation (3) was determined. (b) The critical value κ_1^c , decreases with increasing noise level σ . To determine κ_1^c , as a function of σ , a similar simulation protocol as for (a) was used but with an ensemble of 10^3 initial conditions for each $\kappa_1' \in [0.1, 0.128]$ ($\delta\kappa_1' \approx 5.46875 \times 10^{-5}$) and $\sigma \in [10^{-6}, 10^{-2}]$ ($\delta\sigma = 10^{-5}$). For each initial condition, the system was evolved for 10^8 time units, and initial 10^7 time units were discarded as transients. For a given value of σ , the smallest value of κ_1' for which we observed $\bar{x}' > 0.5$ was picked as the actual critical value κ_1^c .

with increasing noise strength (figure 3(b)), thereby allowing System 1’ to earlier enter the post-crisis regime. The post-crisis dynamics showed rare and recurrent high amplitude oscillations like those reported for System 1 in previous studies [17, 18]. These events are mediated by a channel-like structure in state space, through which a trajectory can escape for a long excursion associated with an extreme event. Our results highlight that noise in the pre-crisis regime can facilitate the access of the trajectories to this channel-like structure, thereby in a sense, lowering the critical value. Similar observations were also reported in optical systems where noise induced rogue waves were observed in parameter ranges which were pre-crisis for the equivalent system without noise [24].

Finally, we demonstrate that the predictive information about the impending global bifurcations we considered here is contained in the maximum amplitudes of signals but not in their variance or lag-1 autocorrelations. The latter two are early warning signals that have been frequently considered in the framework of critical slowing down and are expected to increase before a local bifur-

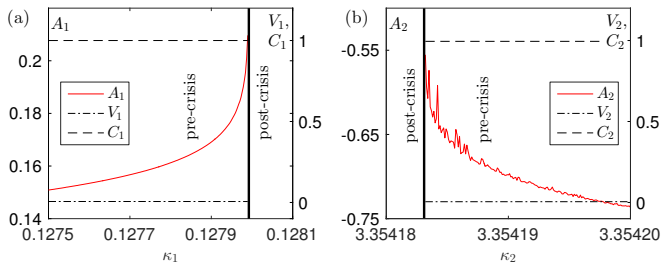


FIG. 4. Maximum amplitudes A_1 and A_2 (red continuous lines) for System 1 (panel (a)) and System 2 (panel (b)) as functions of the control parameters κ_1 and κ_2 , respectively. Variances V_i and lag-1 autocorrelations C_i are shown as dash-dotted and dashed black lines, respectively. For each value of κ_i , V_i and C_i were determined from a single time series of \bar{x} (System 1) and u (System 2), e.g., for System 2, $V_2 = T_2^{-1} \sum_{t=1}^{T_2} (u(t) - \bar{u})^2$, $C_2 = V_2^{-1} T_2^{-1} \sum_{t=1}^{T_2-1} (u(t) - \bar{u})(u(t+1) - \bar{u})$. V_1 and C_1 are defined analogously ($T_1 = 2 \times 10^4$, $T_2 = 10^5$). In each panel, the left ordinate specifies the scale of the maximum amplitudes whereas the right ordinate specifies the scale of the variance and the lag-1 autocorrelation. Black vertical lines mark the locations of the critical values.

cation. In figure 4 (a) and (b), we show the maximum amplitudes A_1 and A_2 for Systems 1 and 2, respectively, prior to the interior crises. In addition, we overlaid these graphs with the variances V_i and lag-1 autocorrelations C_i obtained from observables \bar{x} (System 1) and u (System 2). Approaching the crises, we did not observe V_i and C_i to change drastically and, hence, to indicate any impending transition. We are also not aware of any theoretical argument regarding why both should show changes prior to a crisis. We observed both quantities to stay approximately constant. In contrast, the maximum amplitudes A_i increased prior to the crises—a phenomenon we call *critical attractor growth*—, indicating the impending interior crises.

Why do we observe critical attractor growth in these excitable systems? We hypothesize that the geometric

properties of such systems are the primary reason behind the observed growth in amplitudes. The changes in the alignment of the invariant manifolds with parameter variation (as discussed in previous studies [17, 18]) and the related changes in the flow field patterns allow the trajectories to evolve into the parts of state space which they could not access for parameter values more distant to the crisis, thereby exhibiting the observed growth in maximum amplitudes. We believe that future work that builds upon our findings and provides mathematical results highlighting the mechanisms underlying critical attractor growth has a strong potential to reveal how early warning signals for global bifurcations and other classes of dynamical systems can be derived, thereby increasing the set of critical transitions that can be predicted.

In summary, we introduced an early warning signal that is sensitive to an upcoming global bifurcation, namely an interior crisis in excitable systems. This extends the existing toolbox of early warning signals beyond the prediction of local bifurcations, a need also put forward in previous works [3, 7]. We expect two directions of research to be particularly fruitful: Achieving a theoretical understanding of our early warning signal might pave the way towards the development of signals that are sensitive to even a larger set of global bifurcations. Moreover, for systems moving gradually towards a transition, the development of frameworks that allow to reliably translate early warning signals from monitoring time series into the predictions of points in time at which a transition will occur would be very useful. They would likely open up early warning signals to a plethora of applications, enabling us to be better prepared and to make better informed decisions with respect to impending critical transitions in a variety of dynamical systems that are relevant to human societies.

ACKNOWLEDGMENTS

S.B. acknowledges support by the Volkswagen foundation (Grant No. 88461).

-
- [1] T. M. Lenton, *Nat. Clim. Chang.* **1**, 201 (2011).
 - [2] M. Scheffer, S. R. C. V. Dakos, and E. H. van Nes, *Annu. Rev. Ecol. Evol. Syst.* **46**, 145 (2015).
 - [3] C. Boettiger, N. Ross, and A. Hastings, *Theor. Ecol.* **6**, 255 (2013).
 - [4] T. M. Lenton, *Annu. Rev. Environ. Resour.*, *Annu. Rev. Environ. Resour.* **38**, 1 (2013).
 - [5] C. Trefois, P. M. A. Antony, J. Goncalves, A. Skupin, and R. Balling, *Curr. Opin. Biotechnol.* **34**, 48 (2015).
 - [6] P. Ashwin, S. Wiczorek, R. Vitolo, and P. Cox, *Phil. Trans. R. Soc. A* **370**, 1166 (2012).
 - [7] M. Scheffer, S. R. Carpenter, T. M. Lenton, J. Bascompte, W. Brock, V. Dakos, J. van de Koppel, I. A. van de Leemput, S. A. Levin, E. H. van Nes, M. Pascual, and J. Vandermeer, *Science* **338**, 344 (2012).
 - [8] C. Kuehn, *Physica D: Nonlinear Phenomena* **240**, 1020 (2011).
 - [9] M. Scheffer, J. Bascompte, W. A. Brock, V. Brovkin, S. R. Carpenter, V. Dakos, H. Held, E. H. van Nes, M. Rietkerk, and G. Sugihara, *Nature* **461**, 53 (2009).
 - [10] K. Dai, D. Vorselen, K. S. Korolev, and J. Gore, *Science* **336**, 1175 (2012).
 - [11] S. R. Carpenter, J. J. Cole, M. K. Pace, R. Batt, W. A. Brock, T. Cline, J. Coloso, J. R. Hodgson, J. F. Kitchell, D. A. Seekell, L. Smith, and B. Weidel, *Science* **332**, 1079 (2011).
 - [12] P. D. Ditlevsen and S. J. Johnsen, *Geophysical Research Letters* **37**, L19703 (2010).
 - [13] V. Dakos, S. R. Carpenter, E. H. van Nes, and M. Scheffer, *Philos. Trans. R. Soc. B* **370**, 20130263 (2014).

- [14] C. Grebogi, E. Ott, and J. A. Yorke, *Phys. D Nonlinear Phenom.* **7**, 181 (1983).
- [15] W. L. Ditto, S. Rausedo, R. Cawley, C. Grebogi, G.-H. Hsu, E. Kostelich, E. Ott, H. T. Savage, R. Segnan, M. L. Spano, and J. A. Yorke, *Phys. Rev. Lett.* **63**, 923 (1989).
- [16] A. Roberts, E. Widiasih, M. Wechselberger, and C. K. R. T. Jones, *Physica D: Nonlinear Phenomena* **292-293**, 70 (2015).
- [17] G. Ansmann, R. Karnatak, K. Lehnertz, and U. Feudel, *Phys. Rev. E* **88**, 052911 (2013).
- [18] R. Karnatak, G. Ansmann, U. Feudel, and K. Lehnertz, *Phys. Rev. E* **90**, 022917 (2014).
- [19] C. Grebogi, E. Ott, F. Romeiras, and J. A. Yorke, *Phys. Rev. A* **36**, 5365 (1987).
- [20] G. Ansmann, K. Lehnertz, and U. Feudel, *Phys. Rev. X* **6**, 011030 (2016).
- [21] P. N. Brown, G. D. Byrne, and A. C. Hindmarsh, *SIAM J. Sci. Stat. Comput.* **10**, 1038 (1989).
- [22] A. Witt, U. Feudel, and A. Pikovsky, *Physica D* **109**, 180 (1997).
- [23] Z. A. Thomas, F. Kwasniok, C. A. Boulton, P. M. Cox, R. T. Jones, T. M. Lenton, and C. S. M. Turney, *Climate of the Past* **11**, 1621 (2015).
- [24] J. Zamora-Munt, B. Garbin, S. Barland, M. Giudici, J. R. R. Leite, C. Masoller, and J. R. Tredicce, *Phys. Rev. A* **87**, 035802 (2013).